https://doi.org/10.1016/j.proeng.2017.05.033

Available online at www.sciencedirect.com

ScienceDirect

Procedia Engineering 00 (2017) 000–000

Procedia Engineering

www.elsevier.com/locate/procedia

Transportation Geotechnics and Geoecology, TGG 2017, 17-19 May 2017, Saint Petersburg, Russia

Improved Performance of Ballasted Rail Tracks using Plastics and Rubber Inclusions

Buddhima Indraratna[a], Ngoc Trung Ngo[a], and Cholachat Rujikiatkamjorn[a]*

[a]*Centre for Geomechanics and Railway Engineering, University of Wollongong, Northfields Ave, Wollongong NSW 2522, Australia*

Abstract

Current railroads require significant upgrading to meet the challenges of heavier loads at higher speeds. Due to excessive track degradation, the Australian rail industry spends large amounts on frequent track repair and maintenance, as well as ground improvement prior to track construction where soft and saturated subgrade soils pose considerable difficulties in design and construction. Moreover, the degradation of ballast particles under impact loading seriously hampers the safety and efficiency of rail tracks, which leads to speed restrictions and more frequent track upgrading. Hence, there is a need for innovative design solutions that can extend the service life of tracks to cater for faster and heavier train traffic. The use of planar geosynthetics and recycled rubber mats placed at the interface of ballast and subballast layer has proven an effective approach to mitigate ballast degradation and improve track longevity. This paper presents the current state-of-the-art knowledge of rail track geomechanics conducted at the University of Wollongong (UOW) including topics relating to laboratory testing and computational modeling approaches. The load-deformation responses of rubber mat/geogrid-stabilised ballast are studied in the laboratory using a large-scale drop weight impact testing facility, and Track Process Simulation Apparatus (TPSA). Numerical modelling using discrete element methods (DEM) are used to model geogrid-reinforced ballasted tracks, capturing both the discrete nature of ballast subject to various types of loading and boundary conditions. These results provide promising approaches to incorporate into the existing track design routines catering for future high speed and heavy haul trains.

Peer-review under responsibility of the scientific committee of the International conference on Transportation Geotechnics and Geoecology.

Keywords: Ballast; Geosynthetics; Discrete Element Modelling

* Corresponding author. Tel.: +61 2 4221 3046; fax: +61 2 4221 3238.
E-mail address: indra@uow.edu.au; trung@uow.edu.au

1877-7058
Peer-review under responsibility of the scientific committee of the International conference on Transportation Geotechnics and Geoecology.

1. Main text

Ballasted track is the traditional railway system where the ballast layer provides structural support against the high dynamic stresses transmitted from moving trains. The ever increasing congestion of highway traffic due to the increasing population and rapid urbanisation has highlighted the need for the sustainable development of railroad transportation infrastructure [1, 2]. The ballast layer consists of free-draining granular material acting as a load-bearing layer in rail tracks. The major functions of ballast are: (i) transmitting induced loads to sub-layers at reduced and acceptable stress levels, (ii) providing lateral resistance and (iii) facilitating free drainage conditions [2, 3]. Subject to repeated train passes the granular substructure layers of ballast and subballast often undergo significant deformation under the high cyclic stresses exerted by increasingly heavier and faster trains. This substructure response presents challenges to the track designer and subsequent maintenance upon construction [4-7]. As trains pass over the tracks, ballast aggregates spread laterally due to inadequate confining pressure from the shoulder ballast and also deteriorate due to breakage of angular corners and sharp edges. As a result, the ballast becomes fouled, less angular, and its shear strength is reduced. A large proportion of track maintenance costs is related to problems with the track substructure such as ballast breakage, fouling, poor drainage, differential settlement, and track buckling [8-11].

The use of planar geosynthetic products (i.e. geogrids, geotextiles or geocomposites) has attracted attention because they are economical and relatively easy to install. Past studies have demonstrated that geogrid reinforcement reduces the settlement and degradation of ballast [12-17]. Placing geosynthetics under the ballast confines the aggregates via interlock or frictional resistance among ballast particles which then stiffens the surrounding aggregates and increases the shearing resistance of the composite system. This results in a more resilient long term performance of rail track, as well as helping with drainage and reducing ballast degradation. The ability of geogrids to provide additional confinement to track substructures was noted by Han *et al.* [13] and Rujikiatkamjorn *et al.* [11] where their studies indicate that the interaction between ballast and geogrid is one of the governing parameters controlling the performance of geogrids in ballasted tracks. Recently, the adoption of recycled rubber mats to improve ballasted track has become increasingly popular [6]. These artificial inclusions are known as Under Ballast Mats (UBM), and they produce a relatively soft interface with the ballast and thus decrease internal contact stresses within the ballast. There has been limited comprehensive studies of the geotechnical behaviour of ballast under cyclic and impact loading where resilient rubber mats were installed in ballast [18, 19]. This paper briefly reviews some of the recent research work undertaken on ballast using the state-of-the-art large-scale testing facilities designed and built at the University of Wollongong and discrete element modelling of geogrid-reinforced ballast.

2. Laboratory investigation

2.1. Drop-weight impact testing apparatus

Impact loads caused by wheel or track irregularities (e.g. wheel flats, turnouts, crossings, rail corrugations etc.) accelerate ballast breakage leading to the adverse performance of ballasted rail tracks [20]. In addition, at transition points such as approaches to a bridge or crossing, the change in track stiffness induces high impact forces contributing to excessive settlement [5, 21]. The UOW large scale drop-weight impact testing apparatus comprising a 600 kg hammer free-falling up to 6 m (Fig. 1a) was used to examine the effect of impact loads on ballast deformation. The hammer was lifted mechanically to the required drop height and released by an electronic quick release system. Impact forces were measured by a dynamic load cell (1200 kN capacity) installed on the drop-weight hammer. A piezoelectric accelerometer (10,000 g capacity, where g is the gravitational acceleration) was used to record transient accelerations. Ballast specimens with 300 mm height and diameter were tested. Details of material specifications and test procedures were presented by Nimbalkar et al. [22, 23]. To mimic low confinement in the field, tests were confined in a rubber membrane thick enough to prevent piercing by sharp particles during testing (tensile strength = 600 kN/m^2, tensile strain at failure = 80%, modulus at 10% compressive strain = 3800 kN/m^2). A rigid circular steel plate (thickness, t = 50 mm) was used to represent a stiff subgrade (i.e. bridge deck), where a thin layer of compacted sand was used to simulate relatively weak subgrade conditions.

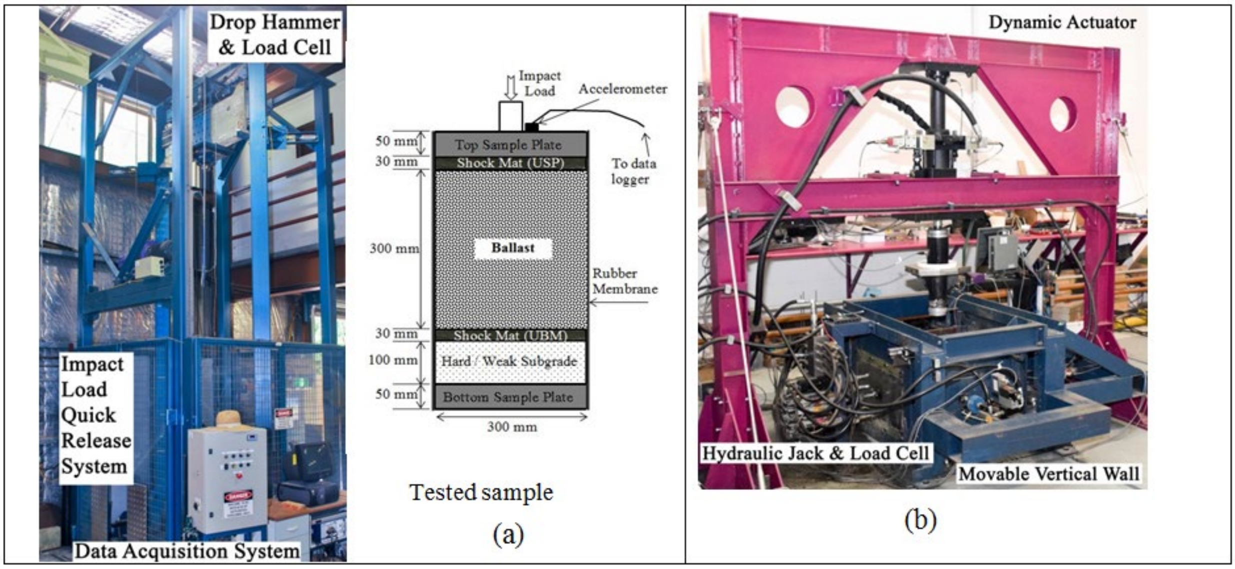

Fig. 1. (a) drop-weight impact apparatus (modified after Kaewunruen and Remennikov (2009); (b) Track Process Simulation Apparatus

Two types of distinct force peaks were measured during the tests, (i) an instantaneous sharp peak with very high frequency termed P_1; (ii) a gradual peak of smaller magnitude with relatively lesser frequency termed P_2.The impact force P_1 is due to the inertia of the rail and sleepers resisting the downward motion of the wheel, and this leads to compression of the contact zone between the wheel and rail. The force P_2 prevails over a longer duration and is attributed to the mechanical resistance of the track substructure leading to its significant compression [24]. These forces will depend on the characteristics of both train and track substructure including relative mass, velocity, contact zone stiffness, loading frequency, and internal energy-absorbing zones. These impact loads are of high magnitude and very short duration depending on the nature of wheel/rail irregularities and on the dynamic response of the track [19, 24, 25].

Force P_2 directly influences the degradation of ballast grains and is calculated as per Australian standards (RIC 2002) by:

$$P_2 = P_0 + 2\alpha V_m \sqrt{\frac{M_u}{M_u + M_t}} \cdot \left[1 - \frac{C_t \pi}{4\sqrt{K_t\left(M_u + M_t\right)}}\right] \cdot \sqrt{K_t M_u} \quad (1)$$

where, P_0 = maximum static wheel load, M_u = vehicle unsprung mass per wheel (kg), 2α = total dip angle (radians), V_m = maximum normal operating velocity (m/s), M_t = equivalent vertical rail mass per wheel (kg), K_t = equivalent vertical rail stiffness per wheel (N/m) and C_t = equivalent vertical rail damping per wheel (Ns/m).

The impact load-time response subjected to the 1st drop of the free-fall hammer is presented in Fig. 2a where two distinct types of force peaks, P_1 and P_2 are clearly visible. It is seen that multiple P1 type peaks are followed by a distinct P_2 type peak. This shows that the ballast mass stabilises after a certain number of impacts to produce an almost constant P_2. The observed benefits of a rubber mat are twofold: (i) it attenuates the impact force, and (ii) it decreases the impulse frequencies thereby extending the duration of the impact. The shear strain (ε_s) of ballast specimens with and without the inclusion of rubber mats are presented in Fig. 2b. It is seen that the shear strain increases with successive impacts. The inclusion of rubber mats placed at top and bottom of the ballast decreased the shear strain significantly for stiff subgrade but for weaker subgrades, this improvement is less significant.

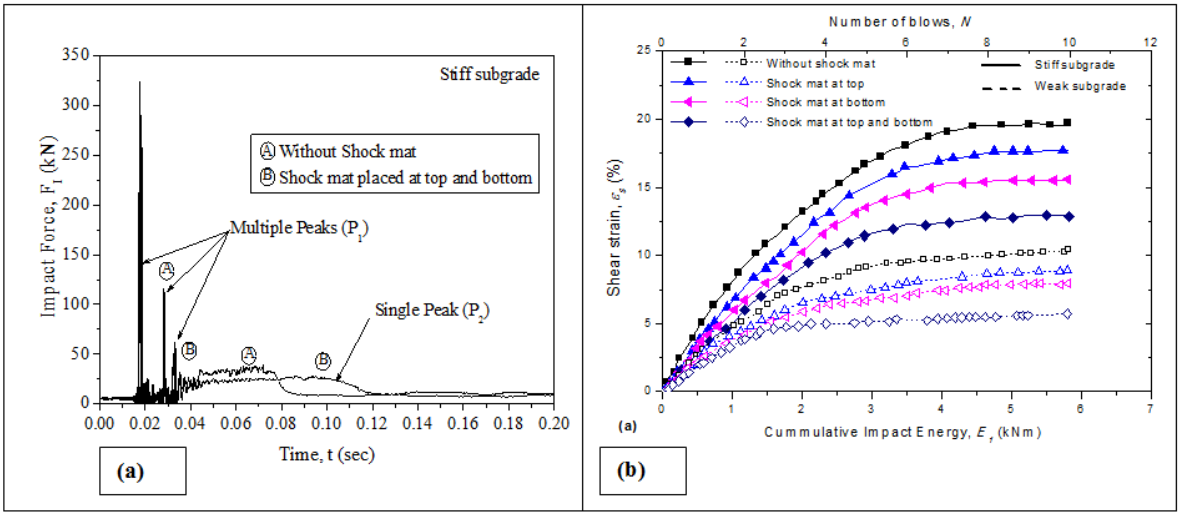

Fig. 2. Impact test results: (a) Impact force responses; (b) Shear strain versus impact energy (*modified after Nimbalkar et al. [22]*)

2.2. Track Process Simulation Apparatus (TPSA)

The cyclic load test corresponded to a 25-ton axle load with a frequency of 15 Hz, simulates a train travelling at about 110 km/h [1]. The servo hydraulic dynamic actuator (Fig. 1b) can replicate the cyclic loading in a sinusoidal wave form with a mean stress of 195 kPa, and amplitude of 165 kPa. Lateral confinement was applied by hydraulic jacks through movable vertical walls that simulated a low confining stress of 10 kPa. A total of a half million load cycles were applied for each cyclic loading test. The TPSA chamber can accommodate a 800×600×600 mm (length×width×height) size sample [17]. The bottom layer of the test specimen was a 150 mm thick compacted layer of subballast. The 300 mm thick layer of ballast above the subballast was compacted by a padded rubber hammer into three equal 100 mm thick layers to achieve a typical field density of 15.3 kN/m3. A 150 mm thick layer of crib ballast was filled around the rail-sleeper assembly and on top of the ballast layer. Fresh and coal fouled ballast samples were prepared following typical gradation curves (e.g. d_{50} = 35 mm, C_u = 1.6). A geogrid reinforcement layer (aperture size: 40 mm x 40 mm) was placed at the ballast-capping. To quantify levels of ballast fouling, the Void Contamination Index (*VCI*) introduced by Tennakoon et al. [8] was used which includes the effect of void ratio, specific gravity and gradation of ballast and fouling material. More details of the TPSA tests can be found at Indraratna et al. [17].

Fig. 3 shows the accumulated settlement of fresh and fouled ballast assemblies with and without geogrid inclusion at varying load cycles. Generally it is seen that the geogrid-reinforced ballast shows reduced settlements compared to the unreinforced assembly for any given *VCI*. As expected, an increased level of fouling results in increased ballast deformation. All samples experience an initial rapid settlement up to 100,000 cycles followed by gradually increasing settlement within 300,000 cycles and then remains relatively stable to the end (500,000 cycles). This clearly indicates that ballast grains undergo considerable rearrangement and densification during initial load cycles [17]. When the ballast grains attain a threshold compression, subsequent loading would resist further settlement but instead promote dilation unless particle crushing occurs [15]. It is seen that the observed benefit of the geogrid decreases with an increase of *VCI* and it becomes marginal when *VCI* > 40%.

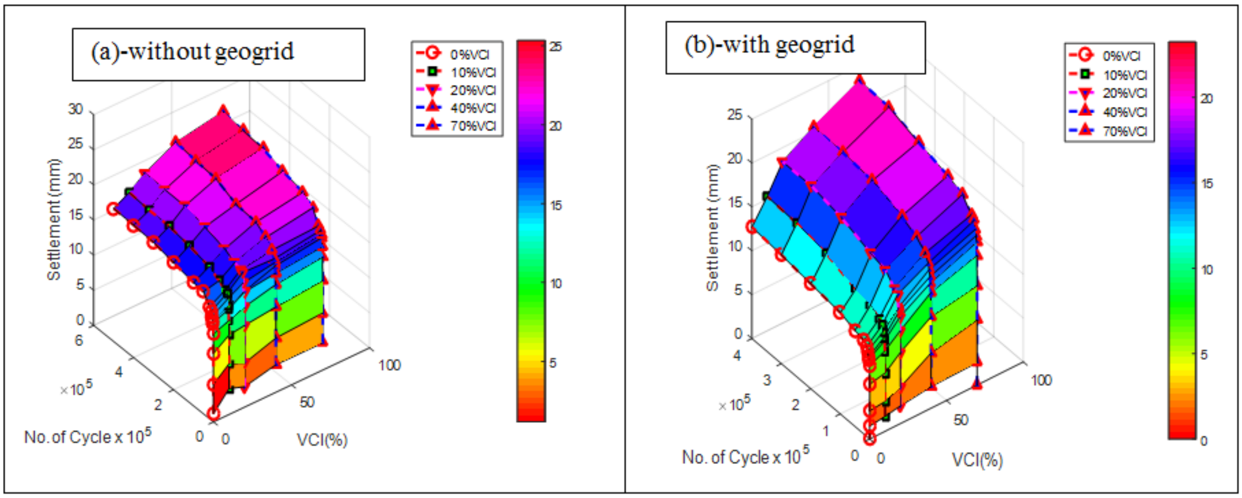

Fig. 3. Measured settlements of fresh and fouled ballast: (a) without geogrid; (b) with geogrid

3. Computational modeling of ballasted tracks

3.1. Discrete Element Method

The discrete element method (DEM) introduced by Cundall and Strack [26] has been used extensively to study the behaviour of granular materials. DEM is often used to model ballast because it captures the discrete nature of a granular assembly which consists of a collection of arbitrarily shaped discrete particles subjected to quasi-static and dynamic conditions [27-31]. Particle motion is determined using Newton's second law and the interaction between particles is determined by contact laws. At a given time, the force

vector $\vec{F}$ that represents the interaction between the two particles is resolved into normal $(\vec{F}_N)$ and shear component $(\vec{F}_T)$ with respect to the contact plane:

$$\vec{F}_N = K_N U^n \quad (2)$$

$$\delta\vec{F}_T = -K_T \cdot \delta U^s \quad (3)$$

where, K_N and K_T are the normal and tangential stiffnesses at the contact; U^n is the normal penetration between two particles; δU^s is the incremental tangential displacement; and $\delta\vec{F}_T$ is the incremental tangential force. The rolling resistance moment $\vec{M}_r$ is introduced to represent the rolling restraint between the two particles A and B and is determined by:

$$\vec{M}_r = \begin{cases} K_r\vec{\omega}_r & if \quad K_r\|\vec{\omega}_r\| < \|\vec{M}_r\|_{lim} \\ \|\vec{M}_r\|_{lim}\frac{\vec{\omega}_r}{\|\vec{\omega}_r\|} & if \quad K_r\|\vec{\omega}_r\| \geq \|\vec{M}_r\|_{lim} \end{cases} \quad (4)$$

where,

$\|\vec{M}_r\|_{lim} = \eta_r\|\vec{F}_r\|\frac{R_A+R_B}{2}$; $K_r = \gamma_r\left(\frac{R_A+R_B}{2}\right)^2$; $\vec{\omega}_r$ is a rolling angular vector representing the relative orientation change between two particles and is computed by adding the angular vectors of the incremental rolling; η_r is the dimensionless coefficient; and γ_r is the rolling resistance coefficient

3.2. Modelling direct shear tests in DEM

Fig. 4 shows how DEM is used to model geogrid-reinforced ballast in a direct shear test. Model dimensions are similar to those carried out in the laboratory (300 mm length x 300 mm width x 200 mm height). Ballast particles with varying shapes and sizes were simulated by clumping many spheres together to represent actual ballast gradation (Fig.4a). This method is widely used to simulate ballast aggregates [24], which are then placed at random locations within the specified wall boundary without overlapping. The micromechanical parameters used to model ballast, geogrid and coal fines are adopted from Ngo et al. [14].

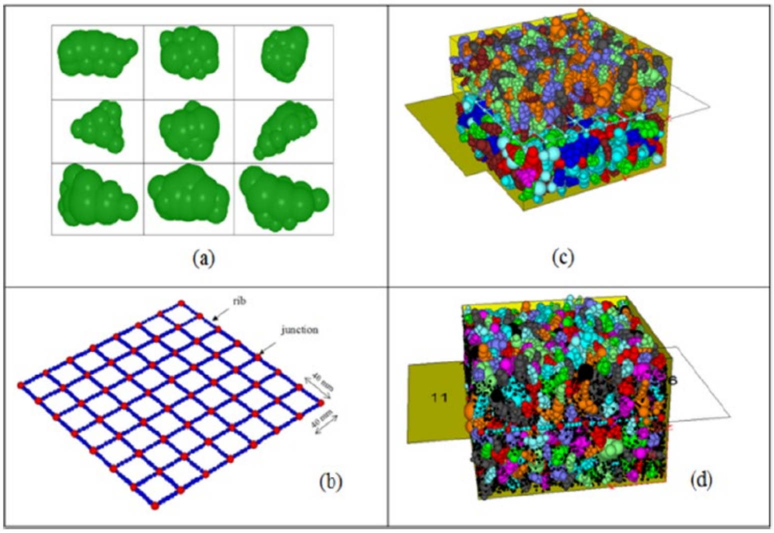

Fig. 4. DEM model of geogrid-reinforced ballast: (a) ballast grains; (b) geogrid; (c) fresh ballast; and (d) fouled ballast

DEM simulations of direct shear tests were conducted at three normal stresses of σ_n = 27kPa, 51kPa, and 75kPa for fresh and fouled ballast (*VCI*=40%) with and without the inclusion of geogrid. Fouling was modelled by the injection of a predetermined number of 1.5 mm spheres (145,665 spheres for *VCI*=40%) into the voids of fresh ballast. Fig. 5 shows comparisons of the shear stress-strain behaviour of geogrid-reinforced ballast from the DEM analysis and those measured experimentally. Note that the simulation results agree reasonably well with the laboratory data for a given normal stress and level of fouling. The strain softening behaviour of ballast and volumetric dilation is observed in all the simulations and show that the higher the normal stress (σ_n), the greater the shear strength and the smaller the dilation. The ability of geogrid reinforcement to increase the shear strength of fresh and fouled ballast can be seen by comparing it with an assembly with unreinforced ballast. This is believed to be due to the interlocking effect that occurs between the ballast grains and geogrid [14].

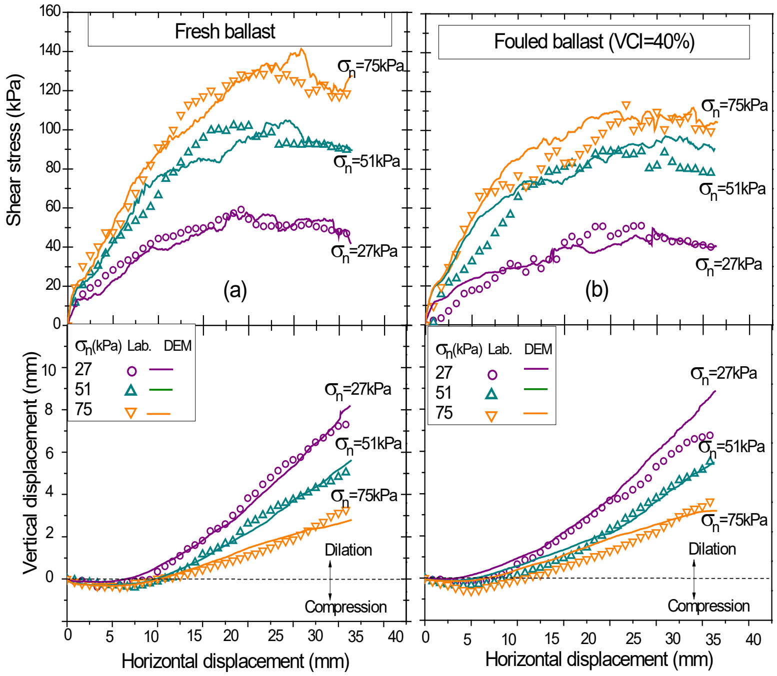

Fig. 5. Comparisons of shear stress-strain of geogrid-reinforced ballast between laboratory test and DEM: (a) fresh ballast; and (b) fouled ballast (modified after Ngo *et al. [14]*)

Load transfer in a ballast assembly depends on the contact force distributions developed across the aggregates through an interconnected network of force chains at contact points [32]. Under a shearing load these contact forces develop and evolve so that the number of load-carrying contacts and their orientations inevitably vary to carry induced stresses. Fig. 6 shows distributions of contact force chains of fresh and fouled ballast (*VCI*=40%) with and without geogrid reinforcement under a given normal stress of 51 kPa, at a shear displacement of Δh= 18 mm. The contact forces between the aggregates are shown as lines whose thickness is proportional to the magnitude of the force. Note that fouled ballast has denser contact chains and less maximum force than those in the fresh ballast assembly. This can be attributed to fine particles clogging the pore spaces between the large grains and partially supported and transmitted forces across the assembly.

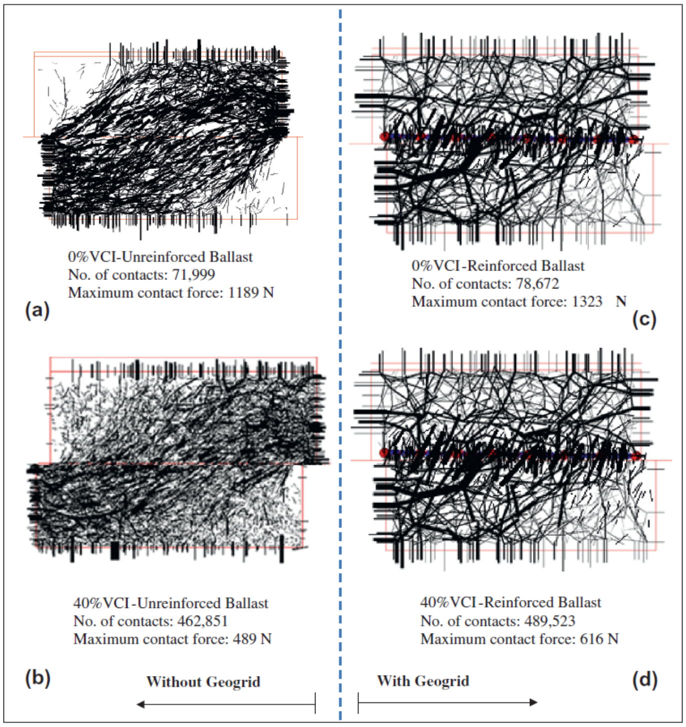

Fig. 6. Distributions of contact forces: (a) unreinforced-fresh ballast; (b) 40%VCI-unreinfoced ballast; (c) geogrid-reinforced fresh ballast; (d) geogrid reinforced fouled ballast (*modified after Ngo et al. [14]*)

4. Conclusions

This paper briefly reviewed the extent of our knowledge of rail track geomechanics resulting from tests and DEM modelling carried out at the UOW. The use of geosynthetics and rubber mats to enhance the performance of rail tracks has been reviewed including large-scale laboratory testing and approaches to computational modelling. A series of tests using the TPSA and impact testing apparatus were conducted to study the role played by geosynthetics and rubber mats in relation to the stress-strain and degradation response of ballast under cyclic and impact loads. Dynamic impact testing indicated that impact loads cause most of the damage to the ballast, and substantial reduction in shear strains and particle breakage can be achieved by using rubber mats. DEM simulations for large-scale direct shear tests were conducted for fresh and fouled ballast (*VCI*=40%) to examine how geogrids improve the performance of ballast. The findings of these studies provide a better understanding of ballast-geogrid interface mechanism, long-term deformation, and degradation, as well as the benefits of using geosynthetics and rubber mats to enhance the performance of ballasted tracks.

Acknowledgements

A number of research projects on ballasted tracks and geosynthetics have been supported in the past and present by the Australian Research Council (ARC). Keen collaborations with industry partners have facilitated the application of theory to practice. In this respect, I sincerely thank Rail Manufacturing CRC (Project R2.5.1), Australasian Centre for Rail Innovation, Tyre Stewardship Australia, Enviro Rubber, Sydney Trains, ARTC. Much of the contents have also been elaborated in past issues of the ASCE Journal of Geotechnical & Geoenvironmental Engineering, Computers and Geotechnics, Int. J. of Geomechanics, among others. Salient contents from these past articles have been reproduced here with kind permission from the original sources.

References

[1] Indraratna, B., Salim, W. and Rujikiatkamjorn, C. (2011a). Advanced Rail Geotechnology - Ballasted Track, CRC Press, Taylor & Francis Group, London, UK

[2] Selig, E.T. and Waters, J.M. (1994). Track geotechnology and substructure management, Thomas Telford, London.

[3] Ngo, N.T. and Indraratna, B. (2016). "Improved performance of rail track substructure using synthetic inclusions: Experimental and numerical investigations." International Journal of Geosynthetics and Ground Engineering, 2(3), pp: 1-16.

[4] Tutumluer, E., Huang, H. and Bian, X. (2012). "Geogrid-aggregate interlock mechanism investigated through aggregate imaging-based discrete element modeling approach." International Journal of Geomechanics, 12(4), pp: 391-398.

[5] Le Pen, L., Watson, G.V.R, Powrie, W., Yeo, G., Weston, P. and Roberts, C. (2014). The behaviour of railway level crossings: Insights through field monitoring, Transportation Geotechnics, 1(4), 201-213.

[6] Nimbalkar, S. and Indraratna, B. (2016). "Improved performance of ballasted rail track using geosynthetics and rubber shockmat." Journal of Geotechnical and Geoenvironmental Engineering, 142(8), pp: 04016031.

[7] McDowell, G.R., Harireche, O., Konietzky, H., Brown, S.F. and Thom, N.H. (2006). "Discrete element modelling of geogrid-reinforced aggregates." Proceedings of the ICE - Geotechnical Engineering 159(1), pp: 35-48.

[8] Tennakoon, N., Indraratna, B., Rujikiatkamjorn, Nimbalkar, and Neville, T. (2012). "The Role of Ballast-Fouling Characteristics on the Drainage Capacity of Rail Substructure." Geotechnical Testing Journal, 35(4), pp: 1-11.

[9] Qian, Y., Han, J., Pokharel, S.K. and Parsons, R.L. (2010). "Experimental study on triaxial geogrid-reinforced bases over weak subgrade under cyclic loading." GeoFlorida 2010: Advances in Analysis, Modeling & Design (Geotechnical Special Publication, 199), ASCE, pp: 1208-1216.

[10] Huang, H. and Tutumluer, E. (2011). "Discrete Element Modeling for fouled railroad ballast." Construction and Building Materials, 25, pp: 3306-3312.

[11] Rujikiatkamjorn, C., Indraratna, B, Ngo, N.T, and Coop, M. (2012). "A laboratory study of railway ballast behaviour under various fouling degree'. Proc., Geosynthetics Asia 2012: 5th Asian Regional Conference on Geosynthetics, Dec. 13-15, Thailand, 2012, pp. 507-514.

[12] Bathurst, R.J. and Raymond, G.P. (1987). "Geogrid reinforcement of ballasted track." Transportation Research Record, 1153, pp: 8-14.

[13] Han, J., Bhandari, A. and Wang, F. (2011). "DEM analysis of stresses and deformations of geogrid-reinforced embankments over piles." International Journal of geomechanics, ASCE, 12(4), pp: 340-350

[14] Ngo, N.T., Indraratna, B. and Rujikiatkamjorn, C. (2014). "DEM simulation of the behaviour of geogrid stabilised ballast fouled with coal." Computers and Geotechnics, 55, pp: 224-231.

[15] Indraratna, B., Ngo, N.T. and Rujikiatkamjorn, C. (2011b). "Behavior of geogrid-reinforced ballast under various levels of fouling." Geotextiles and Geomembranes, 29(3), pp: 313-322.

[16] Biabani, M.M., Indraratna, B. and Ngo, N.T. (2016). "Modelling of geocell-reinforced subballast subjected to cyclic loading." Geotextiles and Geomembranes, 44(4), pp: 489-503.

[17] Indraratna, B., Ngo, N.T. and Rujikiatkamjorn, C. (2013). "Deformation of coal fouled ballast stabilized with geogrid under cyclic load." Journal of Geotechnical and Geoenvironmental Engineering, 139(8), pp: 1275-1289.

[18] Costa, P.A., Calçada, R. and Cardoso, A.S. (2012). "Ballast mats for the reduction of railway traffic vibrations. Numerical study." Soil Dynamics and Earthquake Engineering, 42(0), pp: 137-150.

[19] Ngo, N.T. and Indraratna, B. (2016). "Improved performance of rail track substructure using synthetic inclusions: Experimental and numerical investigations." International Journal of Geosynthetics and Ground Engineering, 2(3), pp: 1-16.

[20] Anastasopoulos, I., Alfi, S., Gazetas, G., Bruni, S. & Leuven, A.V. 2009. Numerical and experimental assessment of advanced concepts to reduce noise and vibration on urban railway turnouts. Journal of Transportation Engineering, ASCE 135(5): 279-287.

[21] Ngo, N.T., Indraratna, B. and Rujikiatkamjorn, C. (2017). "Stabilisation of track substructure with geo-inclusions – experimental evidence and DEM simulation." International Journal of Rail Transportation. DOI: http://dx.doi.org/10.1080/23248378.2017.1279085

[22] Nimbalkar, S., Indraratna, B., Dash, S. and Christie, D. (2012). "Improved performance of railway ballast under impact loads using shock mats." Journal of Geotechnical and Geoenvironmental Engineering, ASCE, 138(3), pp: 281-294.

[23] Kaewunruen, S. and Remennikov, A.M., (2009). Dynamic crack propagations in prestressed concrete sleepers in railway track systems subjected to severe impact loads. Journal of Structural Engineering, 136(6), pp.749-754.

[24] Frederick, C.O. & Round, D. J. 1985. Vertical Track Loading, Track Technology, Thomas Telford Ltd, London.

[25] Jenkins, H.M., Stephenson, J.E., Clayton, G.A., Morland, J.W. & Lyon, D. 1974. The effect of track and vehicle parameters on wheel/rail vertical dynamic forces. Railway Engineering Journal 3: 2-16.

[26] Cundall, P.A. and Strack, O.D.L. (1979). A discrete numerical model for granular assemblies. Geotechnique, 29(1), pp: 47-65.

[27] McDowell, G.R. and Bolton, M.D. (1998). "On the micromechanics of crushable aggregates." Geotechnique, 48(5), pp: 667-679.

[28] McDowell, G.R., Harireche, O., Konietzky, H., Brown, S.F. and Thom, N.H. (2006). "Discrete element modelling of geogrid-reinforced aggregates." Proceedings of the ICE - Geotechnical Engineering 159(1), pp: 35-48.

[29] O'Sullivan, C., Cui, L. and O'Neill, C. (2008). "Discrete element analysis of the response of granular materials during cyclic loading." Soils and Foundations, 48(4), pp: 511-530.

[30] Indraratna, B., Ngo, N.T., Rujikiatkamjorn, C. and Vinod, J. (2014). "Behaviour of fresh and fouled railway ballast subjected to direct shear testing - a discrete element simulation." International Journal of Geomechanics, ASCE, 14(1), pp: 34-44.

[31] Ngo, N.T., Indraratna, B. and Rujikiatkamjorn, C. (2017). "Simulation ballasted track behavior: numerical treatment and field application." International Journal of Geomechanics, 0(0), pp: 04016130. DOI: http://dx.doi.org/10.1061/(ASCE)GM.1943-5622.0000831

[32] McDowell, G.R. and Bolton, M.D. (1998). "On the micromechanics of crushable aggregates." Geotechnique, 48(5), pp: 667-679.